

Technical and Theoretical Analysis of HTS Machines and Their Development

Lu Hai Zheng¹, Jian Xun Jin¹, You Guang Guo², Jian Guo Zhu²

¹School of Automation Engineering,

University of Electronic Science and Technology of China, ChengDu, SiChuan, China 610054

²Faculty of Engineering, University of Technology, Sydney, NSW 2007, Australia

Abstract

Since 1990s, high temperature superconducting (HTS) machine techniques have been gradually developed. The developed HTS machines mainly include DC machines, synchronous machines, induction machines, linear machines, reluctance machines, hysteresis machines, and permanent machines. From the beginning of this century, the HTS machines have made rapid developments and significant achievements. HTS motors and generators are summarized in this paper with regard to their developments, advantages and prospect applications.

Keywords: High temperature superconductor (HTS), HTS machines, HTS rotating motors, HTS generators, HTS linear motor.

1. Introduction

Since 1986, the discovery of high critical temperature superconductors (HTSs) has unfolded the new prospect for the superconducting machine practical applications. Early 1987, as an example, American Electric Power Research Institute (EPRI) entrusted Reliance Electric Corp. (REC) to conduct feasibility study of the motors constructed with HTS materials [1]. At the beginning of 1990's, they had successively produced a small HTS DC motor and 2-5 horsepower (hp) HTS synchronous motors [2,3]. So far, America has already developed a 5 MW (6,500 hp) HTS synchronous motor [4] and 100 MVA HTS synchronous generator [5]. Now, a 36.5 MW (49,000 hp) HTS synchronous motor is being fabricated [6], and will be completed at the end of 2006. Furthermore, a few countries also have developed different types of HTS machines, such as linear, reluctance, hysteresis, and permanent motors [7-19].

This paper introduces the HTS machine developments; and the technical and theoretical analysis of the HTS machines will also be presented.

2. HTS rotating machines

At present HTS rotating machines are in the focus enabling a wide spectrum of power varying from industrial drives of some MW for motor to several hundreds of MVA for large generators and speed ranging from the slow motion of wind power generators or of high-torque ship drives to high-speed generators coupled to gas turbines. The technical and theoretical analysis of various HTS rotating motors and generators will be introduced as follows.

2.1. HTS rotating motors

2.1.1. HTS direct current motors

The research focus of HTS machines was on the HTS DC motor in early days, particularly was the homopolar DC motor used for ship propulsion which has the merits to build conventional electric propulsion ships having greater power, lighter weight and smaller size; and creates a solution for construction of a high speed, low noise warships.

In 1992, EPRI cooperated with REC manufactured a small scale 25 W HTS DC motor [2]. The field winding constitutes of two BSCCO HTS coils, which were dipped into liquid nitrogen tank while working. The two coils survived almost 50 thermal cycles from room temperature to liquid nitrogen temperature without significant degradation of their superconducting properties with the motor operating at its rated output power.

In 1995, United States Naval Surface Warfare Center (NSWC) developed a HTS homopolar DC motor [20] with the field winding construct with BSCCO HTS wire. The motor produced 125 kW (167 hp) of output power with its HTS field winding operating in liquid helium at a temperature of 4.2 K, and produced 91 kW (122 hp) of output power with the field winding cooled by liquid neon to a temperature of 28 K.

In the middle of 1990s, collaboration between the Naval Research Laboratory (NRL) and NSWC, along with industrial partners American Superconductor Corp. (AMSC) and Intermagnetics General Corp. (IGC), had been established in order to produce HTS motors for ship propulsion. In 1998, they had already tested a homopolar DC motor wound from coils of $\text{Bi}_2\text{Sr}_2\text{Ca}_2\text{Cu}_3\text{O}$ tapes [21], which generated the following hp as a function of temperature: 240 kW (320 hp) at 4.2 K, 172 kW (230 hp) at 27 K, and 78 kW (104 hp) at 77 K.

In 2002, a program was underway at General Atomics (GA) for the Office of Naval Research (ONR) where a 3.7 MW HTS homopolar DC motor was developed [22], and with projections for a 19 MW level machine.

2.1.2. HTS synchronous motors

Along with the development of HTS technology and the performance enhancement of HTS material, as well as the maturity of high efficiency power electronics device and the alternating current (AC) speed-adjustment technology of motor, the superconducting AC electric propulsion also obtain people's favor, the most universal form of HTS AC motor is the HTS synchronous motor.

America, Germany, Korea and some other countries have developed a series of HTS synchronous motors in different scales, and focused on the large-scale ship propulsion HTS motors. Table 1 summarizes the main HTS synchronous motors developed.

The major components of HTS-based propulsion synchronous motors are illustrated schematically in Fig. 1. The stator assembly includes the following

- a) AC stator winding;
- b) Back iron;
- c) Stator winding support structure;
- d) Bearing and housing.

The field winding consists of several HTS coils that are conduction-cooled through the support structure. The primary components of the rotor assembly are as follows

- a) HTS field winding operating at 32 K;
- b) Rotor support structure;
- c) Cooling loop;
- d) External cryocooler module, connected to the motor at the non-drive end of the shaft that cools the field winding;
- e) Room-temperature electromagnetic (EM) shield;
- f) Torque tube for transferring torque from the "cold" (cryogenically-cooled) environment to the "warm" shaft ends.

The HTS field winding is an assembly containing multiple polesets, each fabricated using HTS wire that

is designed to withstand the powerful magnetic and mechanical forces experienced in the rotor.

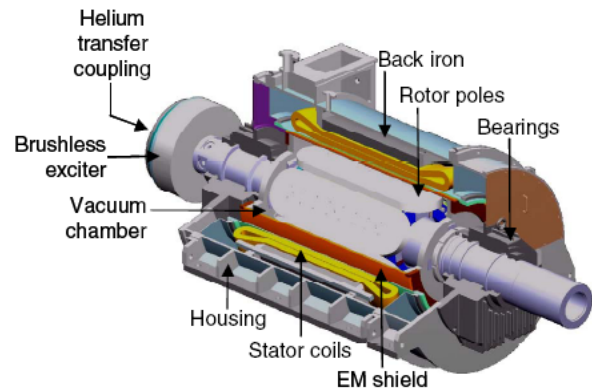


Fig. 1. A HTS synchronous motor concept [6].

The polesets and support structure are enclosed in a vacuum sealed cryostat that minimizes radiant heat input and provides the insulated operating environment required by the HTS field coils.

An EM shield, which is located at the outside surface of the cryostat, directly transfers torque to the warm shaft, and is designed to be mechanically robust to withstand the large forces generated during faults, and is also designed to absorb heating caused by negative sequence currents and any other harmonic currents generated by a variable speed drive.

A refrigeration system, which uses cold circulating helium gas in a closed loop, maintains the HTS field winding at cryogenic temperature. Helium gas is circulated through cooling channels located inside the rotor. The closed cooling loop runs from the turning rotor body to externally located, stationary Gifford-McMahon (GM) cold heads.

The stator winding employs no magnetic iron teeth, because the stator winding bore surface experiences a high magnetic field that would saturate the iron teeth of a conventional stator. With no iron teeth in the winding region, the support and cooling of the stator coils require special attention. Generally, the stator coils employ copper litz conductor, which is made up of small diameter insulated and transposed wire strands.

A 5 MW HTS motor demonstration unit [4] was delivered to the U.S. Navy in July 2003 after factory test. Since from August 2004, the motor was tested in a simulated ship system at Center for Advanced Power Systems (CAPS) at the Florida State University where it was load tested to 5 MW with coupled to two 2.5 MW induction motors is shown in Fig. 2 at the CAPS facility.

For additional specialized testing for the 5 MW motor, it was delivered to NSWC in Philadelphia in August 2005. These cumulative positive test results achieve yet another important benchmark in the development of HTS rotating machinery, and provide important validation for the follow-on U.S. Office of

Naval Research Program, in which a 36.5 MW (49,000 hp), 120 rpm HTS motor currently under construction will be delivered to the U.S. Navy at the end of 2006. A conceptual picture of the 36.5 MW, 120-rpm HTS motor is shown in Fig. 3.

Table 1. HTS Synchronous motors developed.

Contribution	Rated power	Time	Basic parameter	HTS material
America	1.5 kW(2 hp) [3]	1993	2-pole, 3,600 rpm	Multifilamentary BSCCO coil
	3.7 kW(5 hp) [3]	1993	4-pole, 1,800 rpm	Multifilament BSCCO coil
	92 kW(125 hp) [23]	1995	4-pole, 1,800 rpm	Multifilamentary Bi-2223/Ag coil
	735 kW(1,000 hp) [24]	2000	4-pole, 1,800 rpm	Multifilamentary BSCCO tape
	3.7 MW(5,000 hp) [25]	2001	4-pole, 1,800 rpm	Multifilamentary BSCCO wire
	5 MW(6,500 hp) [4]	2003	6-pole, 230 rpm	Multifilamentary BSCCO tape
Siemens	36.5 MW (49,000hp) [6]	2006	120 rpm	Multifilamentary BSCCO tape
	400 kW(550 hp) [7]	2001	4-pole, 1,800 rpm	Mg-reinforced Bi-2223/Ag tape
Korea	4 MW(5,500 hp) [8]	2005	2-pole, 3,600 rpm	Bi-2223 tape
	73.5 kW(100 hp) [26]	2002	4-pole, 1,800 rpm	Stainless steel-reinforced Bi-2223 tape
Japan	3 kW(4 hp) [27]	2001	4-pole, 1,800 rpm	Bi-2223/Ag tape
	3.1 kW(4 hp) [28]	2005	8-pole, 720 rpm	Gd-Ba-Cu-O bulk magnet
Finland	1.5 kW(2 hp) [29]	1997	4-pole, 1,500 rpm	Bi-2223/Ag coil



Fig. 2. 5 MW motor coupled to two 2.5 MW load motors at CAPS [6].

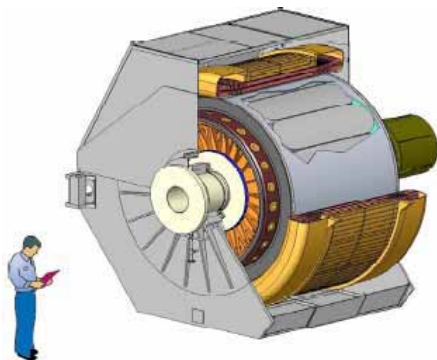


Fig. 3. Conceptual 36.5 MW / 120 rpm motor under construction for delivery to ONR by the end of 2006 [6].

2.1.3. HTS induction motors

Induction motor is well known to be widely utilized in a capacity range from fractional horsepower to large capacity motors, and the squirrel cage type induction is a typical type of induction motors.

Performance of squirrel cage inductions, such as, starting torque and efficiency, are influenced by the resistance of short bars. The rotor of a conventional squirrel cage induction motor consists of short bars and short rings made of copper or aluminum, and the resistance of rotor cannot be changed. When the rotor resistance is small, efficiency at full load operation is high, but starting torque is low. When the rotor resistance is large, high starting torque and low efficiency at full load operation is observed.

To improve both characteristics, it is needed to increase rotor resistance at starting and to decrease it at full load operation. If the conventional bars made of copper or aluminum are replaced by HTS tapes, the rotor resistance can be varied to great extends. Because slip is 1 at the starting of induction motors, large current is induced in the rotor circuit and high frequency is applied to the rotor circuit. These large current and high frequency make HTS tapes quench at the starting of induction motors. Therefore high starting torque can be obtained.

As the speed of rotor builds up, HTS tapes which are used as short bars become superconducting state again because current and frequency of the rotor circuit decrease. After the HTS tapes recover from quench,

resistance of the rotor circuit is completely zero if the joint resistance between short bars and short rings is neglected. In that case, power loss in rotor circuit which is generated in conventional induction motors is eliminated.

In 2003, J. Sin et al from Korea developed a 0.75 kW HTS squirrel cage induction motor [10,30]. The end rings and short bars of rotor were made of Bi-2223 HTS tapes. Stator of the conventional induction motor was used as the stator of the HTS motor. Fig. 4 shows the squirrel cage rotor with HTS wire and overview of the HTS induction motor. To simplify the cooling system of the HTS motor, whole motor including stator and rotor was put in the cryostat and immersed in liquid nitrogen. The HTS induction motor can provide high starting torque and the high efficiency at the same time, and its speed can maintain synchronous speed up to 63 % of rated load. Starting torque of the HTS motor was more than two times of the conventional motor.

In 2006, T. Nakamura et al from Japan developed a HTS squirrel cage induction motor with HTS rotor and conventional stator [31], which is similar to that have developed by J. Sin et al. They also developed the analysis code based upon the electrical equivalent circuit, and explain the mechanism of performance synchronism based on the material property of Bi-2223/Ag multifilamentary tapes and YBCO coated conductor [31,32].

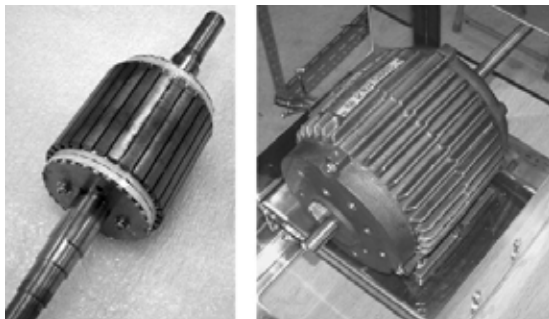


Fig. 4. Overview of the HTS squirrel cage rotor and the motor [10].

2.1.4. Other types of HTS rotating motors

Other types of HTS rotating motors contain hysteresis, reluctance and permanent (trapped field) motors with the rotors containing HTS bulks. These HTS motors are developed on the basis of the theoretical analysis of electrodynamic and hysteresis properties of the HTS YBCO bulk samples and tape shape Bi-2223/Ag elements. The construction scheme of these types of HTS motors is shown in Fig. 5.

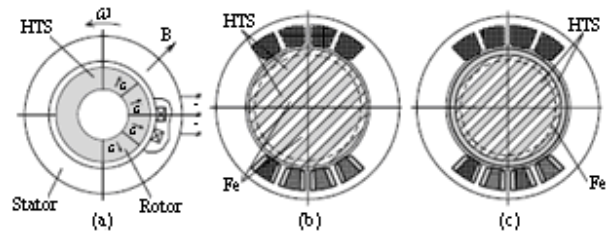


Fig. 5. Schematics of HTS motors, (a) Hysteresis HTS motor, (b) Reluctance HTS motor with compound rotor, (c) Permanent (trapped field) HTS motor [13].

In Russia, Moscow State Aviation Institute (MAI) cooperate with IPHT (Germany) have designed and built series of HTS hysteresis, reluctance and permanent (trapped field) motors [12,13] with output power rating 5-150 kW by using HTS bulk YBCO and Bi-2223/Ag tape elements. These HTS motors have overall dimensions and specific power up to 3-6 times better compared with traditional asynchronous motors and have high power factor.

In 1997, Japan constructed a HTS quasi-permanent motor [33], which reached the values of 2 kW at 77 K. The highest flux density of 2.1 T was achieved at the surface of the YBCO bulk when magnetized by pulsed field magnetization at 30 K by using a cryocooler. In 2001, Japan fabricated an axial-type BSCCO-bulk HTS hysteresis motor [34]. The armature windings supplied electric current from a three-phase PWM inverter. Experimental results of the laboratory-made HTS hysteresis motor were unsatisfactory because of many elements needed to be improved in fabrication.

In 2000, Institute of Electrical Engineering of Chinese Academy of Sciences manufactured a small 2-pole, 1,500 rpm HTS permanent motor [16]. In 2004, they designed and fabricated a 3-phase, 150 W, 2-pole HTS bulk reluctance prototype motor [15].

2.2. HTS rotating generators

Since 2004, General Electric (GE), in conjunction with the US Department of Energy, has manufactured and tested of a 100 MVA class HTS demonstrator generator [5,35]. The commercial HTS utility-size generator has been developed based on GE's iron core superconducting generator technology. The iron core concept has significant advantages over air core designs. The rotor consists of a cold superconducting field coil and coil supports and a warm iron core, which takes the torque and transmits to the shafts.

In 2002, England developed a 3-phase, 100 kVA, 2-pole HTS synchronous generator, operating in the temperature range 57-77 K using liquid coolants down

to 65 K and 57 K, as its sketch shown in Fig. 6 [36]. The rotor was designed with a magnetic core (invar) to reduce the magnetizing current and the field in the coils. Two fiberglass (G10) torque tubes were designed and manufactured to provide the mechanical support required and to reduce the heat intake into the generator cold space.

In 2003, Australia and New Zealand developed a 2 MW, 20 rpm low-speed and high-torque HTS turbine generator [9]. The design features is a multi-pole permanent magnet rotor with a single global HTS stator coil having 4 and 6 m diameter for each phase. This concept minimizes the rotor and machine mass, avoids the need to refrigerate rotating HTS components

and accommodates the limits in bending strain of HTS tapes. The downside of this arrangement is the potential AC losses because the HTS conductor carries AC current and is exposed to alternating magnetic fields.

In 2000, Korea developed a 2 kVA HTS induction generator [11]. The generator had two rotors, inner rotor and outer rotor. The outer rotor was made of copper shell and rotated at a higher angular velocity than that of the rotating magnetic field generated by the stator, but the inner rotor had HTS bulk and rotated in the same angular velocity with the stator field.

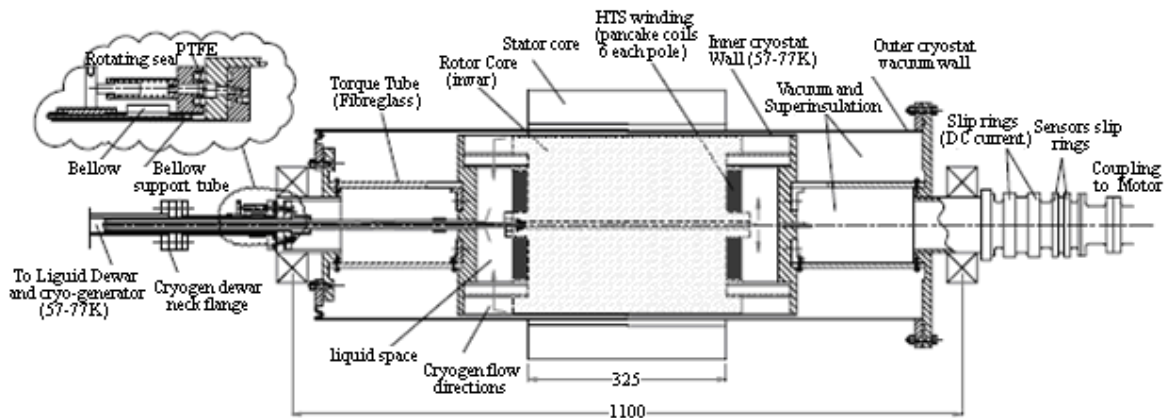


Fig. 6. The sketch of 100 kVA HTS generator [36].

3. HTS linear motors

Since the HTS technology has achieved a fast development as well as a great progress on the HTS materials applied to conventional rotating machines [4-6], applying the HTS materials into the linear motors becomes attractive. Now, some model HTS linear motors (HTSLM) have been designed in some countries like America and Japan, and experience on the HTSLM technology has been well obtained. Theoretical analysis of the HTS levitation properties has been conducted, which provides a theoretical base for the practical development of the HTS linear motors [37]. The development of HTSLM in recent years is introduced as follows.

3.1. HTS single-sided linear actuator

In 2000, Japan Waseda University designed and fabricated a HTS bulk single-sided linear actuator [17],

which can realize levitation and propulsion. The primary and the secondary of the linear actuator were composed of copper windings with iron core and HTS bulks, respectively. As shown in Fig. 7, permanent magnets, the same pole in longitudinal direction, and the alternating poles of N and S in transverse direction, are located at both sides of the primary windings to levitate and guide the secondary. Two types of HTS bulks were used in the linear actuator. A zero-field-cooled HTS bulk plate was located at the centre of the secondary to generate thrust, and four field-cooled HTS bulks located above the permanent magnets play a role of levitation and guidance of the secondary.

In order to improve the linear actuator, the starting thrust force and magnetic field distribution in the air gap was measured, and a simulation program was developed based on the finite element method (FEM) taking the voltage-current (E - J) characteristics of the HTS bulk into consideration to investigate electromagnetic behaviors within the bulk exposed to a

time-varying magnetic field. Using the simulation program, the dependency of n -value and critical current density (J_c) of the bulk material on the magnetic flux density in the air gap and the starting thrust force was investigated. Experiments have good agreements with analyses, and the conclusions are given as follows: The characteristics of a HTS bulk linear actuator are almost independent on the HTS bulk J_c and n -value; both of the magnetic flux density beneath the bulk and the starting thrust increase with n -value and decrease with J_c ; and the influence of J_c on the thrust force was much greater than that of n -value. Based on the numerical analysis results of magnetic flux density and thrust force, a larger n -value is preferable for the linear actuator.

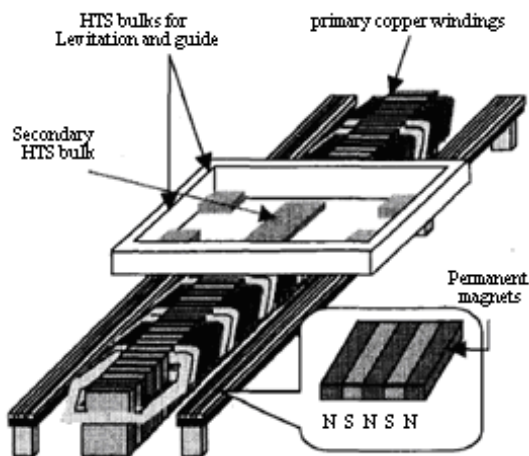


Fig. 7. Experimental setup of linear actuator [17].

3.2. HTS double-sided linear actuator

In 2002, Japan Waseda University constructed a double-sided and short-secondary type of linear synchronous actuator [18,38] with a field-cooled YBCO bulk plate as the secondary, as the structure shown in Fig. 8. The primary can be divided into two sections: (i) The starting section in which the secondary was accelerated as an induction machine; and (ii) The synchronous section in which the secondary moved with a specified synchronous speed. The secondary of the linear actuator consisted of two plate-shaped field-cooled YBCO bulks had some intervals and two copper plates placed at both sides of the YBCO bulks. To move the secondary smoothly, bearings were attached on both sides of the secondary. The YBCO bulk was immersed in a liquid nitrogen (LN_2) bath during experiments.

The primary windings were excited by DC power sources so that a momentary sinusoidal travelling field was formed in the air gap, and the synchronous thrust force can be measured by a load cell which was connected to the secondary. They prepared two special power sources for the starting section and the synchronous section individually. The starting section of the primary was energized by a high-frequency source in the range of 50-100 Hz and the synchronous section was energized by a low-frequency source with 2 Hz.

Important conclusions have been drawn through the experiments and the simulations, and which are significant for designing HTSLM with larger propelling forces. The main conclusions are (i) Thrust force was influenced by load angle, spacing and size of two YBCO bulks. Thrust force was changed sinusoidal when load angle shifts from 0 to 360 degrees, and peak of thrust force shifted from 60 to 120 degrees as decreasing the interval of two bulks from 28 mm to 2 mm. The maximum of the thrust force decreased mostly linearly as the interval of the bulks becomes large. The thrust force of the single 56 mm large bulk was twice as great as that in two 28 mm bulks. (ii) While the secondary can be pulled into synchronism in the case of interval was very small such as 2 mm, it was failed in the case of big interval such as 28 mm. (iii) The amplitude of speed became larger with increasing the thrust force.

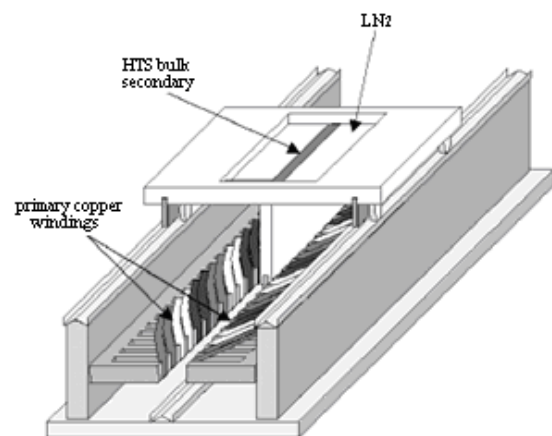


Fig. 8. Schematic drawing of a model linear actuator [38].

3.3. Linear bulk superconducting magnet synchronous motor

In 2004, America designed and fabricated a linear bulk superconducting magnet synchronous motor (LBSCMM) for an electromagnetic aircraft launch

system (EMALS) [39]. The permanent magnets used in conventional design of linear permanent magnet synchronous motors were replaced by the HTS bulk magnets. The complete motor consisted of four independent motors, and each of the four motors was closed loop controlled and supplied by an independent converter. In the case of fault the motor associated with the fault was switched off, and the remaining three motors were sufficient to produce the required thrust force of 2 MN to finish the launch process. One of the motors is shown in Fig. 9, and the coordinate z is assumed to be the direction of motion.

(i) Flux density distribution. The flux density distribution produced by a bulk superconductor (BSC) was determined numerically by the “sand-pile model” in combination with the Biot–Savart law. The sand-pile model of the BSC is schematically shown in Fig. 10.

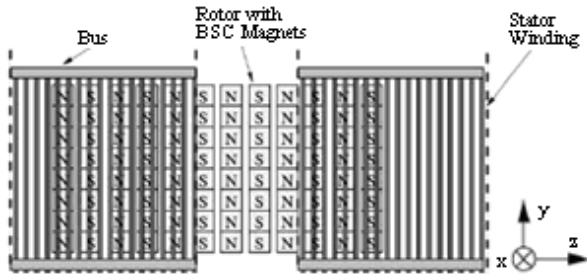


Fig. 9. One motor of the complete LBSCMM [39].

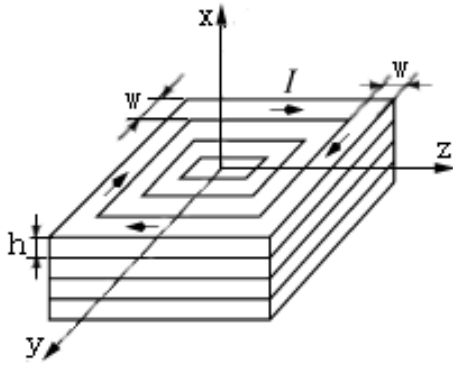


Fig. 10. Sand-pile model of a BSC [39].

It was assumed that the currents flow along the edges so that square current loops were formed; the cross section of each current loop was given by the height h and width w . The current in one current loop was given by

$$I = J_c hw \tag{1}$$

where J_c was the critical current density in the BSC. The complete volume of the BSC was divided into N_L layers with N_C current loops in each layer. Each current loop was approximated with an infinitely thin conductor in the middle of the current loop carrying current I . The differential of flux density vector generated by the current carrying element of conductor dB was given by the Biot–Savart law

$$dB = \frac{\mu_0 I}{4\pi} \frac{1}{\|r\|^3} ds \times r \tag{2}$$

where μ_0 is the permeability of free space, r is the position vector of the current element vector ds to the point of observation. while $\|r\|$ denotes the length of the vector r . The flux density B at the point of observation is calculated by integration along all closed current loops in all layers.

(ii) Force calculation. The force vector dF , acting on an infinite thin stator conductor element vector ds carrying stator current I_s , is given by

$$dF = I_s ds \times B \tag{3}$$

If the stator conductor can not be considered as infinite thin and the flux density vector B is averaged along the axis y , then (3) becomes to

$$dF = J_s Y e_s \times B_{av} dA \tag{4}$$

where B_{av} is the flux density vector averaged with respect to the axis y , J_s is the current density in the stator conductor, Y is the conductor length in the y direction, e_s is the unity vector pointing in the direction of flowing current in the stator conductor, and dA is a differential element of the stator conductor cross section. The total force vector F produced by two poles of the LBSCMM can be calculated by integration over cross sections of all stator conductors.

The physical, operational, and equivalent circuit parameters of the linear motor with HTS bulk magnets have been compared with those of a linear permanent magnet synchronous motor and linear induction motor designed for the same application. Results show that utilizing superconducting magnets is only superior at temperatures below 40 K. It is very likely that technological developments will generate new materials that can trap higher magnetic fields, while the cost of cryogenic operations will continue to be reduced. In this case, the LBSCMM combined with a suitable power electronic converter may be the best candidate for electromagnetic aircraft launch system in a long term.

4. Summary

Progress on HTS development has opened the door to develop HTS motors and generators with potential competitive cost, high efficiency and reliability, and high possibility of acceptance by the end user. The key technologies for development of HTS machines have been essentially proven, and to be sufficiently robust and affordable. With the development and progress of HTS material technology, as well as the realization industrial production of the second generation of HTS wires, HTS machines can be more compact, lighter, and efficient than the conventional machines, and will replace conventional machines in more areas.

5. References

- [1] H.E. Jordan, "Feasibility Study of electric motors constructed with high temperature superconducting materials," *Electric Machines and Power Systems*, vol. 16, no. 1, pp. 15-23, 1989.
- [2] H.J. Chad, and F.S. Rich, "Design and fabrication of high temperature superconducting field coils for a demonstration DC motor," *IEEE Transactions on Applied Superconductivity*, vol. 3, no.1, pp. 373-376, March 1993.
- [3] C.H. Joshi, C.B. Prum, R.F. Schiferl, and D.I. Driscoll, "Demonstration of two synchronous motors using high temperature superconducting field coils," *IEEE Transactions on Applied Superconductivity*, vol. 5, no. 2, pp. 968-971, June 1995.
- [4] S. Greg, G. Bruce, and S.K. Swarn, "The performance of a 5 MW high temperature superconductor ship propulsion motor," *IEEE Transactions on Applied Superconductivity*, vol. 15, no. 2, pp. 2206-2209, June 2005.
- [5] S. Kiruba, H. Xianrui, R. David, W. Konrad, W.B. Jim, T.L. Evangelos, T. Lou, M.F. James, and A. Steve, "AC losses in a high temperature superconducting generator," *IEEE Transactions on Applied Superconductivity*, vol. 15, no. 2, pp. 2162-2165, June 2005.
- [6] S.S. Kalsi, B.B. Gamble, G. Snitchler, and S.O. Ige, "The status of HTS ship propulsion motor developments," *IEEE Power Engineering Society General Meeting*, vol. 18-22, June 2006.
- [7] M. Frank, J. Frauenhofer, P. Van Hasselt, W. Nick, H.W. Neumueller, and G. Nerowski, "Long-term operational experience with first siemens 400 kW hts machine in diverse configurations," *IEEE Transactions on Applied Superconductivity*, vol. 13, no. 2, pp. 2120-2123, June 2003.
- [8] H.W. Neumuller, W. Nick, B. Wacker, M. Frank, G. Nerowski, J. Frauenhofer, W. Rzaeki, and R. Hartig, "Advances in and prospects for development of high-temperature superconductor rotating machines at Siemens," *Superconductor Science and Technology*, vol. 19, no. 3, pp. S114-S117, March 2006.
- [9] M. Fee, M.P. Staines, R.G. Buckley, P.A. Watterson, and J. G. Zhu, "Calculation of AC loss in an HTS wind turbine generator," *IEEE Transactions on Applied Superconductivity*, vol. 13, no. 2, pp. 2193-2196, June 2003.
- [10] J. Sim, M. Park, H. Lim, G. Cha, J. Ji, and J. Lee, "Test of an induction motor with HTS wire at end ring and bars," *IEEE Transactions on Applied Superconductivity*, vol. 13, no. 2, pp. 2231-2234, June 2003.
- [11] S.H. Kim, and S.Y. Hahn, "Analysis and design of a induction generator with a superconducting bulk magnet rotor," *IEEE Transactions on Applied Superconductivity*, vol. 10, no. 1, pp. 931-934, March 2000.
- [12] B. Oswald, M. Krone, T. Strasser, K.J. Best, M. Soll, W. Gawalek, H.J. Gutt, L. Kovalev, L. Fisher, G. Fuchs, G. Krabbes, and H.C. Freyhardt, "Design of HTS reluctance motors up to several hundred kW," *Physica C*, vol. 372-376, pp. 1513-1516, August 2002.
- [13] L.K. Kovalev, K.V. Ilushin, K.L. Kovalev, V.T. Penkin, V.N. Poltavets, S.M.A. Koneev, I. Akimov, W. Gawalek, B. Oswald, and G. Krabbes, "High output power electric motors with bulk HTS elements," *Physica C*, vol. 386, pp. 419-423, April 2003.
- [14] J.X. Jin, Y.G. Guo, and J.G. Zhu, "principle and analysis of a linear motor driver for HTS levitation applications," (M2S06-Id456), *Physica C*, 2007.
- [15] M. Qiu, Z. Xu, Z.H. Yao, D. Xia, L.Z. Lin, G.M. Zhang, L. Xiao, H.T. Ren, Y.L. Jiao, and M.H. Zheng, "Design and performance of a small HTS bulk reluctance motor," *IEEE Transactions on Applied Superconductivity*, vol. 15, no. 2, pp. 1480-1483, June 2005.
- [16] M. Qiu, H.K. Huo, Z. Xu, D. Xia, L.Z. Lin, and G.M. Zhang, "Technical analysis on the application of HTS bulk in "permanent magnet" motor," *IEEE Transactions on Applied Superconductivity*, vol. 15, no. 2, pp. 3172-3175, June 2005.
- [17] R. Muramatsu, S. Sadakata, M. Tsuda, and A. Ishiyama, "Trial production and experiments of linear actuator with HTS Bulk Secondary," *IEEE Transactions on Applied Superconductivity*, vol. 11, no. 1, pp. 1976-1979, March 2001.
- [18] A. Sato, H. Ueda, and A. Ishiyama, "Operational characteristics of linear synchronous actuator with field-cooled HTS bulk secondary," *IEEE Transactions on Applied Superconductivity*, vol. 15, no. 2, pp. 2234-2237, June 2005.
- [19] W.S. Kim, S.Y. Jung, H.Y. Choi, H.K. Jung, J.H. Kim, and S.Y. Hahn, "Development of a superconducting linear synchronous motor," *IEEE Transactions on Applied Superconductivity*, vol. 12, no. 1, pp. 842-845, March 2002.
- [20] J.D. Waltman, and J.M. Superczynski, Jr., "High-temperature superconducting magnet motor demonstration," *IEEE Transactions on Applied*

- Superconductivity, vol. 5, no. 4, pp. 3532-3535, December 1995.
- [21] R.J. Soulen, T.L. Francavilla, D.U. Gubser, D.J. Waltman, N. Sondergaard, and J. Chafe, "Recent developments for ship propulsion using high temperature superconductors," Proc. of the Conference on Cryogenics and Refrigeration, pp. 510-513, 1998.
- [22] R. Thome, W. Creedon, M. Reed, E. Bowles, and K. Schaubel, "Homopolar motor technology development," IEEE Power Engineering Society Transmission and Distribution Conference, vol. 1, pp. 260-264, 2002.
- [23] R.F. Schiferl, B.X. Zhang, D.I. Driscoll, B.A. Shoykhet, and R.C. Dykhuizen, "Development status of a 125 horsepower superconducting motor," Advances in Cryogenic Engineering, Pleunum Press, vol. 42, pp. 977-984, 1997.
- [24] V. Dombrovski, D. Driscoll, B.A. Shoykhet, S.D. Umans, and J.K. Zevchek, "Design and testing of a 1000-hp high-temperature superconducting motor," IEEE Transactions on Energy Conversion, vol. 20, no. 3, pp. 638-643, September 2005.
- [25] B.B. Gamble, S. Kalsi, G. Snitchler, D. Madura, and R. Howard, "The status of HTS motors," Proceedings of the IEEE Power Engineering Society Transmission and Distribution Conference, vol. 1, pp. 270-274, 2002.
- [26] Y.K. Kwon, M.H. Sohn, S.K. Baik, E.Y. Lee, J.M. Kim, T.S. Moon, H.J. Park, Y.C. Kim, and K.S. Ryu, "Development of a 100 hp synchronous motor with HTS field coils," IEEE Transactions on Applied Superconductivity, vol. 15, no. 2, pp. 2194-2197, June 2005.
- [27] Y.S. Jo, Y.K. Kwon, M.H. Sohn, Y.K. Kim, and J.P. Hong, "High temperature superconducting synchronous motor," IEEE Transactions on Applied Superconductivity, vol. 12, no. 1, pp. 833-836, March 2002.
- [28] H. Matsuzaki, Y. Kimura, I. Ohtani, M. Izumi, T. Ida, Y. Akita, H. Sugimoto, M. Miki, and M. Kitano, "An axial gap-type HTS bulk synchronous motor excited by pulsed-field magnetization with vortex-type armature copper windings," IEEE Transactions on Applied Superconductivity, vol. 15, no. 2, pp. 2222-2225, June 2005.
- [29] J.T. Eriksson, R. Mikkonen, J. Paasi, R. Perala, and L. Soderlund, "A HTS synchronous motor at different operating temperatures," IEEE Transactions on Applied Superconductivity, vol. 7, no. 2, pp. 523-526, June 1997.
- [30] J. Sim, K. Lee, G. Cha, and J.K. Lee, "Development of a HTS squirrel cage induction motor with HTS rotor bars," IEEE Transactions on Applied Superconductivity, vol. 14, no. 2, pp. 916-919, June 2004.
- [31] T. Nakamura, H. Miyake, Y. Ogama, G. Morita, I. Muta, and T. Hoshino, "Fabrication and characteristics of HTS induction motor by the use of Bi-2223/Ag squirrel-cage rotor," IEEE Transactions on Applied Superconductivity, vol. 16, no. 2, pp. 1469-1472, June 2006.
- [32] G. Morita, T. Nakamura, and I. Muta, "Theoretical analysis of a YBCO squirrel-cage type induction motor based on an equivalent circuit," Superconductor Science and Technology, vol. 19, no. 6, pp. 473-478, June 2006.
- [33] T. Oka, Y. Itoh, Y. Yanagi, M. Yoshikawa, T. Sakakibara, S. Harada, Y. Yamada, and U. Mizutani, "High temperature superconducting quasi-permanent magnets and their application to superconducting motor," Nippon Kinzoku Gakkaishi/Journal of the Japan Institute of Metals, vol. 61, no. 9, pp. 931-936, September 1997.
- [34] I. Muta, H.J. Jung, T. Hirata, T. Nakamura, T. Hoshino, and T. Konishi, "Fundamental experiments of axial-type BSCCO-bulk superconducting motor model," IEEE Transactions on Applied Superconductivity, vol. 11, no. 1, pp. 1964-1967, March 2001.
- [35] J.M. Fogarty, "Development of a 100 MVA high temperature superconducting generator," 2004 IEEE Power Engineering Society General Meeting, vol. 2, no. 6-10, pp. 2065-2067, June 2004.
- [36] M.K. Al-Mosawi, C. Beduz, K. Goddard, J.K. Sykulski, Y. Yang, B. Xu, K.S. Ship, R. Stoll, and N.G. Stephen, "Design of a 100 kVA high temperature superconducting demonstration synchronous generator," Physica C, vol. 372-376, pp. 1539-1542, August 2002.
- [37] J.X. Jin, "High T_c superconductor theoretical models and electromagnetic flux characteristics," Journal of Electronic Science and Technology of China, vol. 4, no. 3, pp. 202-208, September 2006.
- [38] A. Takahashi, H. Ueda, and A. Ishiyama, "Trial production and experiment of linear synchronous actuator with field-cooled HTS bulk secondary," IEEE Transactions on Applied Superconductivity, vol. 13, no. 2, pp. 2251-2254, June 2003.
- [39] G. Stumberger, M.T. Aydemir, and A.L. Thomas, "Design of a linear bulk superconductor magnet synchronous motor for electromagnetic aircraft launch systems," IEEE Transactions on Applied Superconductivity, vol. 14, no. 1, pp. 54-62, March 2004.

Nature Sciences

Special Issue

*Twenty Years of
High Temperature Superconductivity*



December 2006 Volume 1 No 1

Contents

- 1 – 16 **Twenty Years of High T_c Superconductivity**
By Jian Xun Jin
- 17 – 21 **Deposition of 3-in Double-Sided YBCO Thin Films with Opposite Inverted Cylindrical Guns Sputtering**
By Bowan Tao, Jiajun Chen, Jie Xiong, Yang Qiu, Yin Chen,
Xingzhao Liu, Yanrong Li
- 22 – 26 **Theory of a HTS High Q Electronic Resonator**
By J.X. Jin, C.M. Zhang
- 27 – 32 **DC Power Transmission Analysis with High T_c Superconducting Cable Technology**
By J.X. Jin, C.M. Zhang, Q. Huang
- 33 – 41 **Technical and Theoretical Analysis of HTS Machines and Their Development**
By Lu Hai Zheng, Jian Xun Jin, You Guang Guo, Jian Guo Zhu
- 42 – 47 **Theoretical Models and Analysis of HTS and Magnetic Field Interaction**
By B. Li, J.X. Jin
- 48 – 79 **Practical Applications of High Temperature Superconductors**
By J.X. Jin, L.H. Zheng, R.P. Zhao, J. Zhang, L. Jiang, J.H. Chen,
Y.L. Jiang, H.Y. Zhang

Nature Sciences

Published by
Science Platform Corporation
ACN 118 632 232

Telephone: + 61 2 9630 9002
Editors@naturesciences.org
<http://naturesciences.org>